

# Cross-talk between *Akkermansia muciniphila* and intestinal epithelium controls diet-induced obesity

Amandine Everard<sup>a</sup>, Clara Belzer<sup>b</sup>, Lucie Geurts<sup>a</sup>, Janneke P. Ouwerkerk<sup>b</sup>, Céline Druart<sup>a</sup>, Laure B. Bindels<sup>a</sup>, Yves Guiot<sup>c</sup>, Muriel Derrien<sup>b</sup>, Giulio G. Muccioli<sup>d</sup>, Nathalie M. Delzenne<sup>a</sup>, Willem M. de Vos<sup>b,e</sup>, and Patrice D. Cani<sup>a,1</sup>

<sup>a</sup>Metabolism and Nutrition Research Group, Walloon Excellence in Life sciences and BIOTEchnology (WELBIO), Louvain Drug Research Institute, Université catholique de Louvain, B-1200 Brussels, Belgium; <sup>b</sup>Laboratory of Microbiology, Wageningen University, 6703 HB, Wageningen, The Netherlands. <sup>c</sup>Department of Pathology, Cliniques Universitaires Saint-Luc, Université catholique de Louvain, B-1200 Brussels, Belgium; <sup>d</sup>Bioanalysis and Pharmacology of Bioactive Lipids Research Group, Louvain Drug Research Institute, Université catholique de Louvain, B-1200 Brussels, Belgium; and <sup>e</sup>Departments of Bacteriology and Immunology and Veterinary Biosciences, University of Helsinki, 00014 Helsinki Yliopisto, Helsinki, Finland

Edited\* by Todd R. Klaenhammer, North Carolina State University, Raleigh, NC, and approved March 28, 2013 (received for review November 8, 2012)

**Obesity and type 2 diabetes are characterized by altered gut microbiota, inflammation, and gut barrier disruption. Microbial composition and the mechanisms of interaction with the host that affect gut barrier function during obesity and type 2 diabetes have not been elucidated. We recently isolated *Akkermansia muciniphila*, which is a mucin-degrading bacterium that resides in the mucus layer. The presence of this bacterium inversely correlates with body weight in rodents and humans. However, the precise physiological roles played by this bacterium during obesity and metabolic disorders are unknown. This study demonstrated that the abundance of *A. muciniphila* decreased in obese and type 2 diabetic mice. We also observed that prebiotic feeding normalized *A. muciniphila* abundance, which correlated with an improved metabolic profile. In addition, we demonstrated that *A. muciniphila* treatment reversed high-fat diet-induced metabolic disorders, including fat-mass gain, metabolic endotoxemia, adipose tissue inflammation, and insulin resistance. *A. muciniphila* administration increased the intestinal levels of endocannabinoids that control inflammation, the gut barrier, and gut peptide secretion. Finally, we demonstrated that all these effects required viable *A. muciniphila* because treatment with heat-killed cells did not improve the metabolic profile or the mucus layer thickness. In summary, this study provides substantial insight into the intricate mechanisms of bacterial (i.e., *A. muciniphila*) regulation of the cross-talk between the host and gut microbiota. These results also provide a rationale for the development of a treatment that uses this human mucus colonizer for the prevention or treatment of obesity and its associated metabolic disorders.**

RegIII $\gamma$  | LPS | gut permeability | *Lactobacillus plantarum* | antimicrobial peptides

Gut microbiota were once characterized as bystanders in the intestinal tract, but their active role in intestinal physiology is now widely investigated. In particular, the mutualism that exists between gut microbiota and the host has received much attention. Obesity and type 2 diabetes are characterized by altered gut microbiota (1), inflammation (2), and gut barrier disruption (3–5). We recently demonstrated an association of obesity and type 2 diabetes with increased gut permeability, which induced metabolic endotoxemia and metabolic inflammation (3–5). Unequivocal evidence demonstrates that gut microbiota influence whole-body metabolism (1, 6) by affecting the energy balance (6), gut permeability (4, 5), serum lipopolysaccharides [i.e., metabolic endotoxemia (7)], and metabolic inflammation (3–5, 7) that are associated with obesity and associated disorders. However, the microbial composition and the exact mechanisms of interaction between these two partners that affect host–gut barrier function and metabolism remain unclear.

The intestinal epithelium is the interface for the interaction between gut microbiota and host tissues (8). This barrier is enhanced by the presence of a mucus layer and immune factors that are produced by the host (9). Antimicrobial peptides for innate immunity are produced by Paneth cells (e.g.,  $\alpha$ -defensins, lysozyme C, phospholipases, and C-type lectin, primarily regenerating islet-

derived 3- $\gamma$ , RegIII $\gamma$ ) or enterocytes (RegIII $\gamma$ ) (10–12). Adaptive immune system effectors that are secreted into the intestinal lumen, such as IgA, may also restrict bacterial penetration into the host mucus and mucosal tissue (13). These immune factors allow the host to control its interactions with gut microbiota and shape its microbial communities (11).

The endocannabinoid system has also been implicated in the control of the gut barrier and inflammation (5, 14). One lipid in this system, 2-arachidonoylglycerol (2-AG), reduces metabolic endotoxemia and systemic inflammation (15). Another acylglycerol, 2-palmitoylglycerol (2-PG), potentiates the antiinflammatory effects of 2-AG (16). Importantly, 2-oleoylglycerol (2-OG) stimulates the release of gut peptides, such as glucagon-like peptide-1 (GLP-1) and glucagon-like peptide-2 (GLP-2), from intestinal L-cells (17). These peptides are implicated in the control of glucose homeostasis and gut barrier function, respectively (4).

Recently, *Akkermansia muciniphila* has been identified as a mucin-degrading bacteria that resides in the mucus layer (18), and it is the dominant human bacterium that abundantly colonizes this nutrient-rich environment (18). *A. muciniphila* may represent 3–5% of the microbial community (18, 19) in healthy subjects, and its abundance inversely correlates with body weight (20–23) and type 1 diabetes (24) in mice and humans, although a recent metagenomic study found that some of the genes belonging to *A. muciniphila* were enriched in type 2 diabetic subjects (25).

We recently discovered that the administration of prebiotics (oligofructose) to genetically obese mice increased the abundance of *A. muciniphila* by ~100-fold (23). However, the direct implications of *A. muciniphila* for obesity and type 2 diabetes have not been determined, and the precise physiological roles it plays during these processes are not known.

Our previous results and the close proximity of this bacterium to the human intestinal epithelium support the hypothesis that *A. muciniphila* plays a crucial role in the mutualism between the gut microbiota and host that controls gut barrier function and other physiological and homeostatic functions during obesity and type 2 diabetes. We administered alive or heat-killed *A. muciniphila* to mice that were fed a high-fat diet and investigated the gut barrier, glucose homeostasis, and adipose tissue metabolism to test this hypothesis.

Author contributions: P.D.C. designed research; A.E., C.B., L.G., J.P.O., C.D., L.B.B., M.D., G.G.M., W.M.d.V., and P.D.C. performed research; C.B., J.P.O., Y.G., M.D., G.G.M., N.M.D., W.M.d.V., and P.D.C. contributed new reagents/analytic tools; A.E., C.B., L.G., J.P.O., Y.G., G.G.M., W.M.d.V., and P.D.C. analyzed data; and A.E., C.B., W.M.d.V., and P.D.C. wrote the paper.

The authors declare no conflict of interest.

\*This Direct Submission article had a prearranged editor.

Freely available online through the PNAS open access option.

<sup>1</sup>To whom correspondence should be addressed. E-mail: patrice.cani@uclouvain.be.

This article contains supporting information online at [www.pnas.org/lookup/suppl/doi:10.1073/pnas.1219451110/-DCSupplemental](http://www.pnas.org/lookup/suppl/doi:10.1073/pnas.1219451110/-DCSupplemental).

## Results

**A. muciniphila Abundance Decreased in Obese and Type 2 Diabetic Mice.** We observed that the abundance of *A. muciniphila* was 3,300-fold lower in leptin-deficient obese mice than in their lean littermates (Fig. 1A). We also observed a 100-fold decrease of this bacterium in high-fat-(HF)-fed mice (Fig. 1B).

**Prebiotic Treatment Restored Basal Levels of *A. muciniphila* and Improved Metabolic Endotoxemia and Related Disorders That Are Associated with HF-Diet-Induced Obesity.** Prebiotics (oligofructose) completely restored *A. muciniphila* counts in both models (Fig. 1B and C), therefore supporting the data obtained in our previous study performed in *ob/ob* mice (23). Administration of prebiotics in HF-fed mice abolished metabolic endotoxemia (Fig. 1D) and normalized the CD11c subpopulation of macrophages in adipose tissue, which is the primary population of increased adipose tissue macrophages in obesity (2) (Fig. 1E). Administration of prebiotics also reduced the total fat mass, the mass of the different fat pads (i.e., s.c., mesenteric, and epididymal), and the body weight (Fig. 1F and Fig. S1A–C). These results were significantly and inversely correlated with *A. muciniphila* abundance (Fig. 1G and Fig. S1D and E). However, the role of the lack of *A. muciniphila* in the molecular mechanisms that underlie the onset of these disorders has not been demonstrated, and whether an increased abundance of *A. muciniphila* reverses these disorders must be investigated. *A. muciniphila* was orally administered to control or HF-fed mice for 4 wk to address these questions.

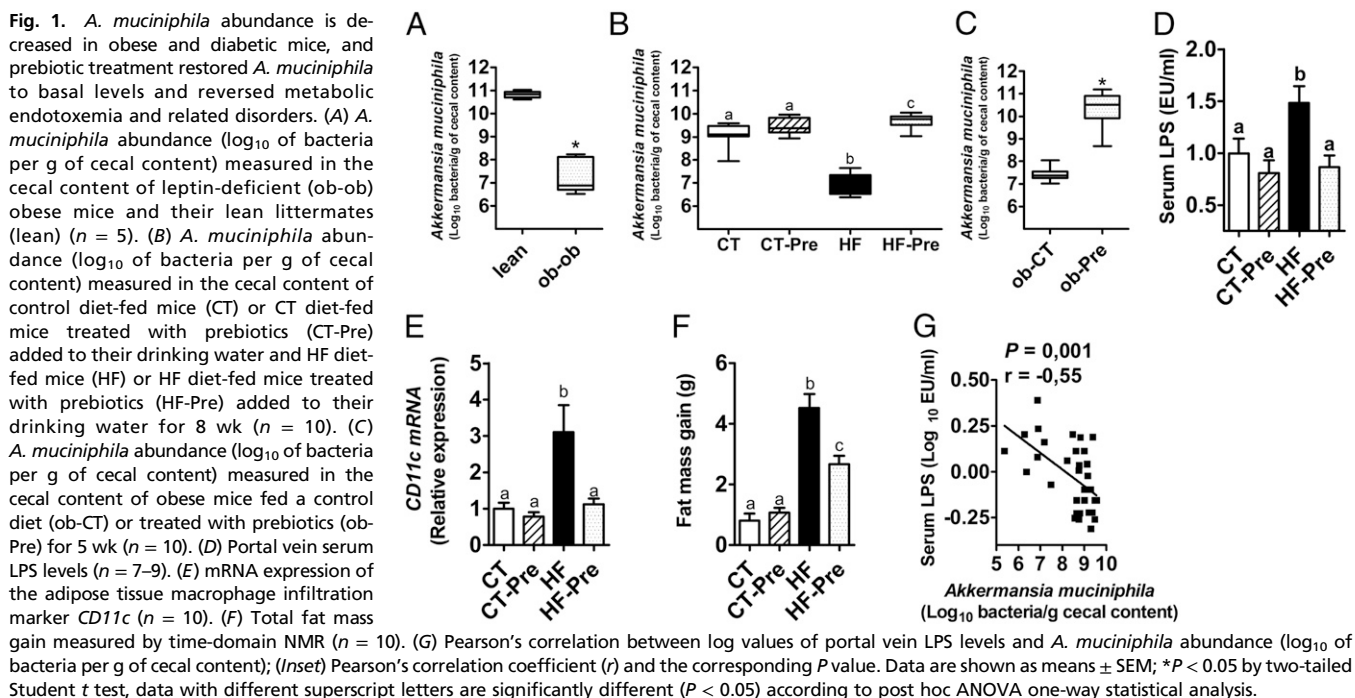
**HF Diet Altered the Gut Microbiota Composition, Whereas *A. muciniphila* Did Not Significantly Induce Changes.** *A. muciniphila* treatment was associated with an increase in *A. muciniphila* abundance in the cecal content of mice (Fig. S2A). We also demonstrated that an HF diet significantly changes the gut microbiota using a phylogenetic microarray (Mouse Intestinal Tract Chip, MITChip) (10, 23), as shown by principal component analyses (Fig. 2A), dendrogram clustering, and representational difference analysis (Fig. S2B and C), whereas *A. muciniphila* treatment did not modify this profile (Fig. 2A and Fig. S2B and C).

## A. muciniphila Improved Metabolic Disorders in Diet-Induced Obese Mice.

*A. muciniphila* treatment normalized diet-induced metabolic endotoxemia, adiposity, and the adipose tissue marker CD11c (Fig. 2B–D and Fig. S3A). Similarly, *A. muciniphila* treatment reduced body weight and improved body composition (i.e., fat mass/lean mass ratio) (Fig. S3B and C) without changes in food intake (Fig. S3D). We demonstrated that *A. muciniphila* treatment completely reversed diet-induced fasting hyperglycemia (Fig. 2E) via a mechanism that was associated with a 40% reduction in hepatic glucose-6-phosphatase expression (Fig. 2F), thereby suggesting a reduction in gluconeogenesis. Notably, the insulin resistance index was similarly reduced after *A. muciniphila* treatment (Fig. S3E). These results suggest a key role for *A. muciniphila* in gut barrier function, metabolic inflammation, and fat storage. Therefore, we hypothesized that *A. muciniphila* would impact adipose tissue metabolism. We demonstrated that *A. muciniphila* treatment under an HF diet increased the mRNA expression of markers of adipocyte differentiation (e.g., CCAAT/enhancer-binding protein- $\alpha$ , encoded by *Cebpa*) and lipid oxidation (e.g., carnitine palmitoyltransferase-1, encoded by *Cpt1*; acyl-CoA-oxidase, encoded by *Acox1*; peroxisome proliferator-activated receptor  $\gamma$  coactivator, encoded by *Pgc1a*; and peroxisome proliferator-activated receptor alpha, encoded by *Ppara*) without affecting lipogenesis markers (e.g., acetyl-CoA carboxylase, encoded by *Acc1* and fatty acid synthase, encoded by *Fasn*) (Fig. 2G). These data further confirm our hypothesis that *A. muciniphila* controls fat storage, adipose tissue metabolism, and glucose homeostasis.

## A. muciniphila Treatment Exerted Minor Effects on Antibacterial Peptide Content in the Ileum and IgA Levels in the Feces.

Recent data suggest that the intestinal mucosa contributes to the maintenance of the gut barrier by secreting antimicrobial peptides for innate immunity that are produced by Paneth cells (e.g.,  $\alpha$ -defensins, lysozyme C, phospholipases, and C-type lectin, primarily the RegIII $\gamma$ ) or enterocytes (RegIII $\gamma$ ) (10, 12). We measured the expression of Paneth and epithelial cell antibacterial markers in the ileum to elucidate the impact of the HF diet and *A. muciniphila* treatment on gut barrier function. *A. muciniphila* increased the



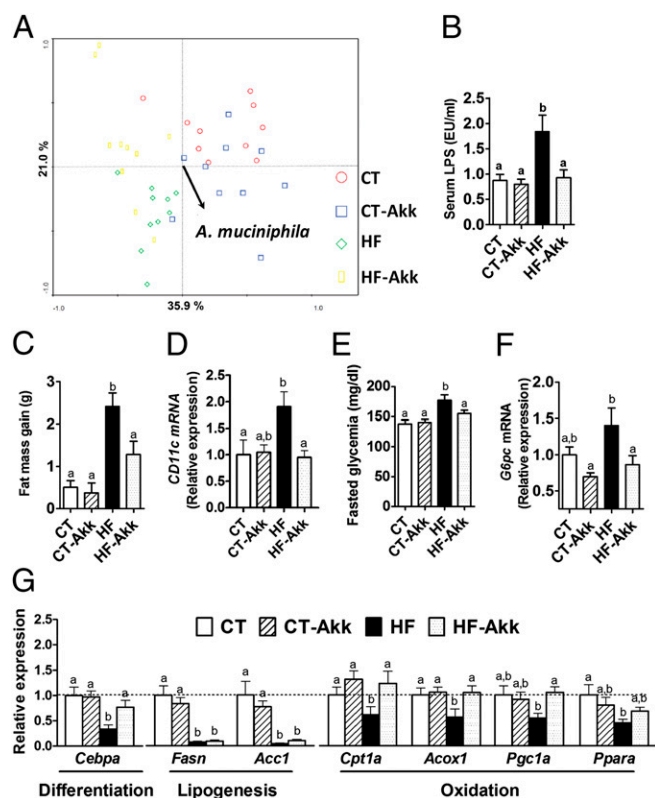


**Fig. 2.** *A. muciniphila* counteracted metabolic endotoxemia, diet-induced obesity, adipose tissue macrophage infiltration, improved glucose homeostasis, and adipose tissue metabolism in diet-induced obese mice without modifying gut microbiota composition. (A) Principal component analysis using the MITChip phylogenetic fingerprints of the gut microbiota from the cecal contents of control mice treated with a daily oral gavage containing sterile anaerobic PBS for 4 wk and fed a control (CT) or HF diet (HF) (CT in red and HF in green) and in mice treated with a daily oral gavage containing *A. muciniphila* ( $2.10^8$  bacterial cells suspended in 200  $\mu$ L of sterile anaerobic PBS) and fed a control (CT-Akk) or HF diet (HF-Akk) (CT-Akk in blue and HF-Akk in yellow) ( $n = 10$ ). (B) Portal vein serum LPS levels ( $n = 6-10$ ). (C) Total fat mass gain measured by time-domain NMR ( $n = 10$ ). (D) mRNA expression of the adipose tissue macrophage infiltration marker *CD11c* ( $n = 10$ ). (E) Fasting glycemia ( $n = 10$ ). (F) Liver *G6pc* mRNA ( $n = 10$ ). (G) mRNA expression of markers of adipocyte differentiation (*Cebpa*), lipogenesis (*Acc1*; *Fasn*), and lipid oxidation (*Cpt1a*; *Acox1*; *Pgc1a*; and *Ppara*) was measured in visceral fat depots (mesenteric fat) ( $n = 10$ ). Data are shown as means  $\pm$  SEM. Data with different superscript letters are significantly different ( $P < 0.05$ ) according to post hoc ANOVA one-way statistical analysis.

expression of *Reg3g* (RegIII $\gamma$ ) under the control diet, but this effect was not observed in HF-fed mice (Fig. S4A). *Pla2g2a* and *Defa* expression were similar between groups, but *Lyz1* expression tended to be lower after bacterial administration (Fig. S4B–D). We also measured IgA in fecal samples as an adaptive immune system factor (13). Fecal IgA levels were not affected by the treatments (Fig. S4E), which suggests that *A. muciniphila* controls gut barrier function by other mechanisms of epithelial signaling (26).

***A. muciniphila* Increased Endocannabinoid (Acylglycerols) Content in the Ileum.** We previously observed a link between gut microbiota and intestinal endocannabinoid system tone (5). We demonstrated an association of decreased monoacylglycerol lipase expression with improved gut barrier function and decreased metabolic inflammation (5). We also demonstrated previously that the pharmacological inhibition of monoacylglycerol lipase reduced metabolic endotoxemia and systemic inflammation (15), which suggests a

direct link between acylglycerols and gut barrier function. Therefore, we measured intestinal acylglycerol levels and demonstrated that *A. muciniphila* treatment increased the levels of 2-OG, 2-AG, and 2-PG (Fig. 3A). These results support a direct link between *A. muciniphila* administration and intestinal levels of acylglycerols that are involved in glucose and intestinal homeostasis.

***A. muciniphila* Counteracted Diet-Induced Colon Mucosal Barrier Dysfunction During Obesity.** Recent evidence supports that interactions between the gut microbiota and mucus layer are dynamic systems that affect mucus barrier biology (9, 27). Therefore, we investigated the impact of *A. muciniphila* treatment on the thickness of the inner mucus layer. We demonstrated a 46% thinner mucus layer in HF-fed mice, and *A. muciniphila* treatment counteracted this decrease (Fig. 3B and C).

**Viable but Not Heat-Killed *A. muciniphila* Counteracted Diet-Induced Metabolic and Mucosal Barrier Dysfunction During Obesity.** To further demonstrate whether *A. muciniphila* has to be alive to exert its metabolic effects, we have compared the impact of viable *A. muciniphila* administration with that of heat-killed *A. muciniphila*. We found that viable *A. muciniphila* counteracted diet-induced metabolic endotoxemia, fat mass development, and altered adipose tissue metabolism (Fig. 4A, B, and D and Fig. S5A) to a similar extent as observed in the first set of experiments (Fig. 2B, C, and G and Fig. S3A). Importantly, these effects were not observed after administration of heat-killed *A. muciniphila* (Fig. 4A, B, and D and Fig. S5A). In addition, we found that viable *A. muciniphila* significantly reduced plasma glucose levels after an oral glucose tolerance test (Fig. 4C), whereas heat-killed *A. muciniphila* exhibited glucose intolerance similar to that of HF-fed mice (Fig. 4C). Finally, we confirmed that viable *A. muciniphila*

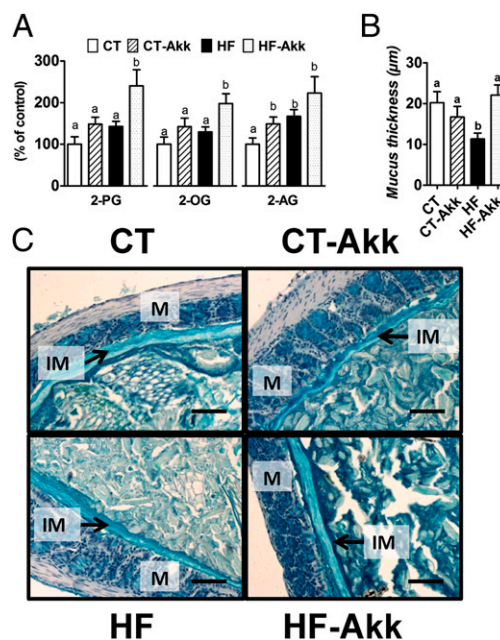


**Fig. 3.** *A. muciniphila* colonization restored gut barrier function and increased intestinal endocannabinoids in diet-induced obese mice. (A) Ileum 2-PG, 2-OG, and 2-AG (expressed as percentage of the control) ( $n = 10$ ). (B) Thickness of the mucus layer measured by histological analyses after alcian blue staining ( $n = 7-8$ ). (C) Representative alcian blue images that were used for mucus layer thickness measurements. M, mucosa; IM, inner mucus layer. (Scale bars, 40  $\mu$ m.) Data are shown as means  $\pm$  SEM. Data with different superscript letters are significantly different ( $P < 0.05$ ) according to post hoc ANOVA one-way statistical analysis.

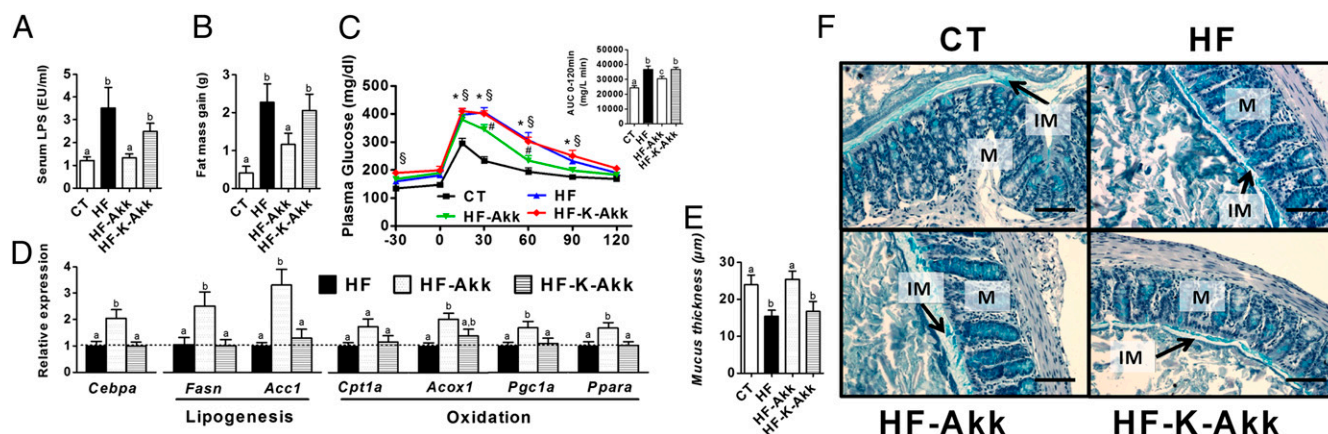


**Fig. 4.** Heat-killed *A. muciniphila* did not counteract metabolic endotoxemia, diet-induced obesity, oral glucose intolerance, and did not improve adipose tissue metabolism and gut barrier function in diet-induced obese mice. Control mice were fed a control (CT) or HF diet (HF) and treated with a daily oral gavage containing sterile anaerobic PBS and glycerol for 4 wk daily. Treated mice received an oral gavage of alive *A. muciniphila* (HF-Akk) or killed *A. muciniphila* (HF-K-Akk) ( $2.10^8$  bacterial cells suspended in 200  $\mu$ L of sterile anaerobic PBS) and fed an HF diet ( $n = 8$ ). (A) Portal vein serum LPS levels ( $n = 6-7$ ). (B) Total fat mass gain measured by time-domain NMR ( $n = 7-8$ ). (C) Plasma glucose profile after 2 g/kg glucose oral challenge in freely moving mice. (Inset) Mean area under the curve (AUC) measured between 0 and 120 min after glucose load ( $n = 7-8$ ). (D) mRNA expression of markers of adipocyte differentiation (*Cebpa*), lipogenesis (*Acc1*; *Fasn*), and lipid oxidation (*Cpt1a*; *Acox1*; *Pgc1a*; and *Ppara*) was measured in visceral fat depots (mesenteric fat) ( $n = 8$ ). (E) Thickness of the mucus layer measured by histological analyses after alcian blue staining (CT  $n = 4$ , HF  $n = 6$ , HF-Akk and HF-K-Akk  $n = 5$ ). (F) Representative alcian blue images that were used for mucus layer thickness measurements. M, mucosa; IM, inner mucus layer. (Scale bars, 40  $\mu$ m.) Data are shown as means  $\pm$  SEM. Data with different superscript letters are significantly different ( $P < 0.05$ ) according to post hoc ANOVA one-way statistical analysis.

restored mucus layer thickness upon HF-diet, whereas we found that heat-killed *A. muciniphila* did not improve mucus layer thickness compared with HF (Fig. 4 E and F). It is worth noting that we found 100-fold more viable *A. muciniphila* recovered from the cecal and colonic content of *A. muciniphila*-treated mice compared with the HF and heat-killed bacteria groups (HF-Akk:  $9.5 \pm 1.02 \log_{10}$  cells/mg of content; HF and HF-K-Akk:  $6.8 \pm 0.51 \log_{10}$  cells/mg of content;  $P = 0.0059$ ), thereby evidencing the viability of *A. muciniphila* after oral administration.

This study confirms that that HF diet-induced obesity is associated with changes in gut microbiota composition (7) (28) (Fig. 2A and Fig. S2 B and C). However, antimicrobial peptides in the ileum were not affected by the treatments. In contrast, *Reg3g* expression in colon epithelial cells was significantly reduced, by  $\sim 50\%$ , in HF and heat-killed *A. muciniphila* treated mice, whereas viable *A. muciniphila* treatment completely blunted this effect and increased *Reg3g* expression upon HF diet (Fig. S5B).

## Discussion

This study demonstrated a dramatic decrease in *A. muciniphila* in genetically and diet-induced obese mice. We demonstrated that prebiotic (oligofructose) treatment restored *A. muciniphila* abundance and improved gut barrier and metabolic parameters. However, the mechanisms that were responsible for the bloom in *A. muciniphila* caused by prebiotic administration are not clear. *A. muciniphila* does not grow on oligofructose-enriched media (in vitro), which suggests that complex cross-feeding interactions contributed to this effect. However, it has been previously shown in rats that oligofructose feeding increases the number of goblet cells and mucus layer thickness (29). Thus, whether oligofructose feeding increases *A. muciniphila* by providing the main source of energy for this bacterium and thereby favoring its growth or whether the increase of *A. muciniphila* increases mucus production and degradation (i.e., turnover) remain to be demonstrated. Oligofructose changes more than 100 different taxa in mice (23). Therefore, we cannot exclude that oligofructose induces specific changes in the gut bacteria and cross-feeding promoting the growth of *A. muciniphila*. In the present study, we investigated the direct impact of *A. muciniphila*. We reversed the pathological phenotype by restoring the

physiological abundance of this strain in obese and diabetic mice. These results demonstrated the key role of *A. muciniphila* in the physiopathology of obesity, type 2 diabetes, and metabolic inflammation. These experiments clearly demonstrate that viable *A. muciniphila* controls gut barrier function, fat mass storage, and glucose homeostasis in obese and type 2 diabetic mice via several mechanisms. These results provide proof of this concept in this context. The major weaknesses in investigations of the role of gut microbiota in the etiology of obesity and type 2 diabetes is the reliance on conclusions that are based on correlative data between bacteria (or one genus) and physiological parameters, because most of the gut bacteria have been identified at the phylogenetic level (i.e., through metagenomic approaches) but have never been cultured.

Several reports have demonstrated the importance of selected bacteria [i.e., *Lactobacillus* spp (30, 31), *Bifidobacterium* spp (32, 33), and *Bacteroides uniformis* CECTT 7771 (34)] on fat mass development during diet-induced obesity, but the aims of these studies were different from that of the present study. These studies investigated the impact of supplementation with one specific probiotic strain or strains that were isolated from healthy infants on physiological parameters. Here we investigated the strain that is affected during obesity and type 2 diabetes in humans and rodents (18, 23). Probiotics have far fewer opportunities for direct contact with the mucosa, but *A. muciniphila* may induces differential host responses because of more intensive contact with the host mucosa (26). To further confirm this hypothesis, we have treated HF-fed mice with a probiotic (i.e., *Lactobacillus plantarum* WCFS1). We found that *L. plantarum* administration did not change fat mass development, adipose tissue metabolism, mucus layer thickness, colon *Reg3g* mRNA, and metabolic endotoxemia (Fig. S6 A-E). Therefore, these data suggest that *A. muciniphila* induces specific host responses compared with other putative beneficial microbes.

*A. muciniphila* is a Gram-negative bacteria (i.e., it contains LPS) that constitutes 3–5% of the gut microbial community. However, our study clearly demonstrated the lack of a direct relationship between the abundance of Gram-negative bacteria within the gut and metabolic endotoxemia (i.e., that is caused by serum LPS) because gut colonization by *A. muciniphila* decreased metabolic endotoxemia arising on an HF diet. One explanation for this

counterintuitive result may be that *A. muciniphila* regulates gut barrier function at different levels. Previous data suggest that gut microbiota contribute to gut barrier alterations during obesity and metabolic endotoxemia (4). However, the different mechanisms of interaction between bacteria and the host that affect gut barrier function during obesity and type 2 diabetes have not been elucidated. This study identified an association of obesity with a decrease in mucus thickness, which supports an additional mechanism of increased gut permeability (i.e., metabolic endotoxemia) that is characteristic of obesity and associated disorders. Furthermore, we demonstrated that *A. muciniphila* restored this mucus layer, which suggests that this mechanism contributes to the reduction in metabolic endotoxemia that was observed during *A. muciniphila* treatment. Moreover, we found that viable *A. muciniphila* induces these effects, whereas heat-killed *A. muciniphila* did not protect the mice from diet-induced obesity and associated disorders.

These results suggest that the presence of viable *A. muciniphila* within the mucus layer is a crucial mechanism in the control of host mucus turnover (19), which improves gut barrier function. However, we cannot exclude additional mechanisms that have been implicated in the regulation of gut barrier. For example, we previously demonstrated that gut microbiota control gut peptides (e.g., GLP-2) that regulate epithelial cell proliferation and gut barrier function (4). Prebiotics stimulate GLP-1 and GLP-2 secretion by acting on the enteroendocrine L-cells that are primarily in the ileum and colon (6). The abundance of *A. muciniphila* is associated with higher L-cell activity (i.e., GLP-1 and GLP-2 secretion) (4, 23), but the mechanisms underlying this relationship are not known. Here, we demonstrated that *A. muciniphila* administration significantly increased intestinal levels of 2-OG, which stimulates glucagon-like peptide secretion from intestinal L-cells (17). Altogether our data suggest that this could be a key mechanism by which *A. muciniphila* controls gut barrier function, metabolic endotoxemia, and metabolism. We also demonstrated that *A. muciniphila* administration increased 2-AG intestinal levels. We recently demonstrated that an increase in 2-AG endogenous levels induced by selective monoacylglycerol lipase inhibitor protects against trinitrobenzene sulfonic acid-induced colitis in mice (15) and reduces metabolic endotoxemia as well as the level of circulating inflammatory cytokines and peripheral and brain inflammation. Therefore, the increased 2-AG levels that were observed after *A. muciniphila* treatment may have also contributed to the reduced inflammation. However, whether the induction of these endocannabinoids after *A. muciniphila* treatment constitutes the molecular event that links these metabolic features warrants further investigation.

Specifically, we demonstrated that the restoration of the physiological abundance of *A. muciniphila* reduced diet-induced body weight gain, fat mass development, and fasting hyperglycemia without affecting food intake. This variation in energy storage is explained by the normalization of adipose tissue adipogenesis (i.e., differentiation and lipogenesis) and fatty acid oxidation. We have previously demonstrated that higher circulating LPS levels inhibit adipose tissue differentiation and lipogenesis, thereby contributing to altered adipose tissue metabolism characterizing obesity (5). Thus, we postulate that *A. muciniphila* restores gut barrier function and thereby contributes to normalize metabolic endotoxemia and adipose tissue metabolism. We found that *A. muciniphila* improved glucose tolerance and decreased endogenous hepatic glucose production. These findings are not in agreement with the apparent but low association of *A. muciniphila* genes with type 2 diabetes-associated metagenome-wide associated studies (25). Nevertheless, the data by Qin et al. remain to be confirmed because this related to only 337 of the 2,176 *A. muciniphila* genes (35) and may be confounded by dietary or pharmaceutical treatments specifically favoring its growth in the human intestine.

Dynamic insulin resistance assessments and the present results suggest improved insulin sensitivity. However, we cannot exclude the possibility that the improvements in glucose and lipid metabolism occurred via an LPS-dependent mechanism, as demonstrated previously (5, 7). We confirmed (7, 36) that an HF diet profoundly affected the gut microbiota composition, whereas *A. muciniphila* administration did not significantly affect this profile. Therefore, it is tempting to extrapolate our findings as a single-species-dependent modulation of the gut microbiota. Moreover, because heat-killing of *A. muciniphila* completely abolished the metabolic effects it is unlikely that specific *A. muciniphila*-derived cell-envelope components may directly contribute to the phenotype observed with viable *A. muciniphila*. It is worth noting that this observation also minimizes the possibility that the host response was caused by a substance in the culture media. However, although not directly fitting with the aim of the present study, follow-up studies of the gut microbiome after viable *A. muciniphila* administration may identify the components that contribute to disease or the host physiological response (37).

Finally, we demonstrated that *A. muciniphila* regulates intestinal antimicrobial peptides in the colon (e.g., RegIII $\gamma$ ). *A. muciniphila* exerted minor effects on antimicrobial peptide production in the ileum. RegIII $\gamma$  exerts direct bactericidal activity against Gram-positive bacteria in the intestine. Therefore, *A. muciniphila* may manipulate host immunity to favor its own survival through an increase in RegIII $\gamma$  expression, which reduces the competition for resources and induces long-term tolerance for the development in the mucus layer. Here, we clearly found that viable *A. muciniphila* significantly increased RegIII $\gamma$ , whereas heat-killed *A. muciniphila* did not affect this parameter. Whether the effect on RegIII $\gamma$  should be considered as beneficial or harmful for the host remain to be determined. These results link the colonization of the colon, but not the ileum, by *A. muciniphila* with the fundamental immune mechanisms through which RegIII $\gamma$  promotes host–bacterial mutualism and regulates the spatial relationships between the microbiota and host (38). Finally, *A. muciniphila* is known to degrade human mucus (18). However, whether the beneficial effects observed here may be extended to other pathological situations in which the mucus layer is altered (e.g., intestinal inflammatory diseases) (39) remain to be elucidated.

We recently demonstrated that germ-free mice that were monoassociated with *A. muciniphila* exhibit important modulations of gene expression; the most marked changes were observed in the colon (442 genes), followed by the ileum (253 genes) and the cecum (211 genes) (26). In the colon, 60 genes, including 16 genes encoding CD antigen markers and 10 genes encoding immune cell membrane receptors, were up-regulated after *A. muciniphila* colonization (26). Several pathways that regulate lipid metabolism, cell signaling, and molecular transport are mostly affected in the ileum (26). These data have uncovered mechanisms of bacterial interaction with the host to control gut permeability and metabolism. Further studies should explore the cellular processes and identify the bacterial products that regulate the host cell responses and metabolic effects of *A. muciniphila*.

In summary, this study provided unique and substantial insights into the intricate regulation of the cross-talk between the host and *A. muciniphila* bacteria. These results provide a rationale for the development of a treatment that uses this human mucus colonizer for the prevention or treatment of obesity and its associated metabolic disorders.

## Materials and Methods

**Mice.** Male C57BL/6 mice were used in the four series of experiments. Cecal contents from genetic (*ob/ob*) and HF-fed obese and type 2 diabetic mice treated or not with prebiotics (oligofructose, 0.3 g per mouse per day) were harvested, immersed in liquid nitrogen, and stored at  $-80^{\circ}\text{C}$  for further *A. muciniphila* analysis. A subset of 10-wk-old C57BL/6J was fed a control diet (CT) or an HF diet (60% fat). The mice were treated with *A. muciniphila*

by oral gavage at a dose of  $2.10^8$  cfu/0.2 mL suspended in sterile anaerobic PBS (CT-Akk and HF-Akk), or heat-killed *A. muciniphila* (HF-K-Akk). Control groups were orally administered an equivalent volume of sterile anaerobic PBS containing a similar end concentration of glycerol (2.5% vol/vol) (CT and HF). Treatments were continued for 4 wk. *A. muciniphila* Muc<sup>T</sup> (ATCC BAA-835) was grown anaerobically in a mucin-based basal medium as described previously (18). The cultures were washed and concentrated in anaerobic PBS that included 25% (vol/vol) glycerol to an end concentration of  $1.10^{10}$  cfu/mL under strict anaerobic conditions. Body composition was assessed using a 7.5-MHz time-domain NMR. Blood, adipose depots, liver, cecal content, and intestinal segments (ileum, cecum, and colon) were collected at death and analyzed. A complete description of the mouse experiments and bacteria preparation is provided in *SI Material and Methods*.

**Gut Microbiota Analysis.** Gut microbiota analyses were performed using real-time quantitative PCR (qPCR) analysis and the MITChip, which is a phylogenetic microarray consisting of 3,580 different oligonucleotide probes that target two hypervariable regions of the 16S rRNA gene (the V1 and V6 regions). Analyses of the MITChip were performed as described previously (23, 40) and in *SI Material and Methods*.

**Gene Expression Analysis.** The expression of metabolic genes of interest and RNA expression profiles were analyzed using real-time qPCR analysis as described in *SI Material and Methods*.

**Measurement of Endocannabinoid Intestinal Levels.** Intestinal endocannabinoids were measured using an LTQ Orbitrap mass spectrometer as described in *SI Material and Methods*.

**Biochemical Analysis.** Plasma insulin and fecal IgA were analyzed using ELISA as described in *SI Material and Methods*. The thickness of the mucus layer was measured in proximal colon segments that were fixed in Carnoy's solution and in 5- $\mu$ m paraffin sections stained with alcian blue as described in *SI Material and Methods*. LPS concentrations in portal vein blood were measured using Endosafe-Multi-Cartridge System based on the limulus amoebocyte lysate kinetic chromogenic methodology as described in *SI Material and Methods*.

**Statistical Analysis.** Data are expressed as means  $\pm$  SEM. Differences between two groups were assessed using the unpaired two-tailed Student *t* test. Data sets that involved more than two groups were assessed using ANOVA followed by Newman-Keuls post hoc tests. Correlations were analyzed using Pearson's correlation. In the figures, data with different superscript letters are significantly different at  $P < 0.05$ , according to post hoc ANOVA statistical analyses. Data were analyzed using GraphPad Prism version 5.00 for Windows (GraphPad Software). The results were considered statistically significant when  $P < 0.05$ .

**ACKNOWLEDGMENTS.** We thank R. M. Goebels for histological assistance, and B. Es Saadi and R. Sellenlagh for technical assistance. P.D.C. is a research associate from the Fonds de la Recherche Scientifique (FRS-FNRS, Belgium) and is the recipient of FSR and FRSM (Fonds Spéciaux de Recherches, Université catholique de Louvain, Belgium; Fonds de la Recherche Scientifique Médicale, Belgium) and Société Francophone du Diabète (France) subsidies. A.E. is a doctoral fellow from the FRS-FNRS. G.G.M. is the recipient of subsidies from the FSR and FRSM and from FRS-FNRS Grant FRFC 2.4555.08. J.P.O. and C.B. were funded by European Research Council Advance Grant 250172-MicrobesInside, awarded to W.M.d.V., whose work was further supported by an unrestricted Spinoza Award of the Netherlands Organization for Scientific Research.

- Turnbaugh PJ, et al. (2006) An obesity-associated gut microbiome with increased capacity for energy harvest. *Nature* 444(7122):1027–1031.
- Osborn O, Olefsky JM (2012) The cellular and signaling networks linking the immune system and metabolism in disease. *Nat Med* 18(3):363–374.
- Cani PD, et al. (2008) Changes in gut microbiota control metabolic endotoxemia-induced inflammation in high-fat diet-induced obesity and diabetes in mice. *Diabetes* 57(6):1470–1481.
- Cani PD, et al. (2009) Changes in gut microbiota control inflammation in obese mice through a mechanism involving GLP-2-driven improvement of gut permeability. *Gut* 58(8):1091–1103.
- Muccioli GG, et al. (2010) The endocannabinoid system links gut microbiota to adipogenesis. *Mol Syst Biol* 6:392.
- Cani PD, Osto M, Geurts L, Everard A (2012) Involvement of gut microbiota in the development of low-grade inflammation and type 2 diabetes associated with obesity. *Gut Microbes* 3(4):279–288.
- Cani PD, et al. (2007) Metabolic endotoxemia initiates obesity and insulin resistance. *Diabetes* 56(7):1761–1772.
- Wells JM, Rossi O, Meijerink M, van Baarlen P (2011) Epithelial crosstalk at the microbiota-mucosal interface. *Proc Natl Acad Sci USA* 108(Suppl 1):4607–4614.
- Johansson ME, Larsson JM, Hansson GC (2011) The two mucus layers of colon are organized by the MUC2 mucin, whereas the outer layer is a legislator of host-microbial interactions. *Proc Natl Acad Sci USA* 108(Suppl 1):4659–4665.
- Bevins CL, Salzman NH (2011) Paneth cells, antimicrobial peptides and maintenance of intestinal homeostasis. *Nat Rev Microbiol* 9(5):356–368.
- Pott J, Hornef M (2012) Innate immune signalling at the intestinal epithelium in homeostasis and disease. *EMBO Rep* 13(8):684–698.
- Hooper LV, Macpherson AJ (2010) Immune adaptations that maintain homeostasis with the intestinal microbiota. *Nat Rev Immunol* 10(3):159–169.
- Macpherson AJ, Geueking MB, Slack E, Hapfelmeier S, McCoy KD (2012) The habitat, double life, citizenship, and forgetfulness of IgA. *Immunol Rev* 245(1):132–146.
- Cani PD (2012) Crosstalk between the gut microbiota and the endocannabinoid system: impact on the gut barrier function and the adipose tissue. *Clin Microbiol Infect* 18(Suppl 4):50–53.
- Alhouayek M, Lambert DM, Delzenne NM, Cani PD, Muccioli GG (2011) Increasing endogenous 2-arachidonoylglycerol levels counteracts colitis and related systemic inflammation. *FASEB J* 25(8):2711–2721.
- Ben-Shabat S, et al. (1998) An entourage effect: Inactive endogenous fatty acid glycerol esters enhance 2-arachidonoyl-glycerol cannabinoic activity. *Eur J Pharmacol* 353(1):23–31.
- Hansen KB, et al. (2011) 2-Oleoyl glycerol is a GPR119 agonist and signals GLP-1 release in humans. *J Clin Endocrinol Metab* 96(9):E1409–E1417.
- Derrien M, Vaughan EE, Plugge CM, de Vos WM (2004) *Akkermansia muciniphila* gen. nov., sp. nov., a human intestinal mucin-degrading bacterium. *Int J Syst Evol Microbiol* 54(Pt 5):1469–1476.
- Belzer C, de Vos WM (2012) Microbes inside—from diversity to function: The case of *Akkermansia*. *ISME J* 6(8):1449–1458.
- Santacruz A, et al. (2010) Gut microbiota composition is associated with body weight, weight gain and biochemical parameters in pregnant women. *Br J Nutr* 104(1):83–92.
- Karlsson CL, et al. (2012) The microbiota of the gut in preschool children with normal and excessive body weight. *Obesity (Silver Spring)* 20(11):2257–2261.
- Collado MC, Isolauri E, Laitinen K, Salminen S (2008) Distinct composition of gut microbiota during pregnancy in overweight and normal-weight women. *Am J Clin Nutr* 88(4):894–899.
- Everard A, et al. (2011) Responses of gut microbiota and glucose and lipid metabolism to prebiotics in genetic obese and diet-induced leptin-resistant mice. *Diabetes* 60(11):2775–2786.
- Hansen CH, et al. (2012) Early life treatment with vancomycin propagates *Akkermansia muciniphila* and reduces diabetes incidence in the NOD mouse. *Diabetologia* 55(8):2285–2294.
- Qin J, et al. (2012) A metagenome-wide association study of gut microbiota in type 2 diabetes. *Nature* 490(7418):55–60.
- Derrien M, et al. (2011) Modulation of mucosal immune response, tolerance, and proliferation in mice colonized by the mucin-degrader *Akkermansia muciniphila*. *Front Microbiol* 2:166.
- Ottman N, Smidt H, de Vos WM, Belzer C (2012) The function of our microbiota: Who is out there and what do they do? *Front Cell Infect Microbiol* 2:104.
- Turnbaugh PJ, Bäckhed F, Fulton L, Gordon JI (2008) Diet-induced obesity is linked to marked but reversible alterations in the mouse distal gut microbiome. *Cell Host Microbe* 3(4):213–223.
- Kleessen B, Hartmann L, Blaut M (2003) Fructans in the diet cause alterations of intestinal mucosal architecture, released mucins and mucosa-associated bifidobacteria in gnotobiotic rats. *Br J Nutr* 89(5):597–606.
- Mohamadzadeh M, et al. (2011) Regulation of induced colonic inflammation by *Lactobacillus acidophilus* deficient in lipoteichoic acid. *Proc Natl Acad Sci USA* 108(Suppl 1):4623–4630.
- Fäk F, Bäckhed F (2012) *Lactobacillus reuteri* prevents diet-induced obesity, but not atherosclerosis, in a strain dependent fashion in ApoE<sup>-/-</sup> Mice. *PLoS ONE* 7(10):e46837.
- Chen JJ, Wang R, Li XF, Wang RL (2011) Bifidobacterium longum supplementation improved high-fat-fed-induced metabolic syndrome and promoted intestinal Reg I gene expression. *Exp Biol Med (Maywood)* 236(7):823–831.
- An HM, et al. (2011) Antiobesity and lipid-lowering effects of Bifidobacterium spp. in high fat diet-induced obese rats. *Lipids Health Dis* 10:116.
- Gauffin Cano P, Santacruz A, Moya A, Sanz Y (2012) Bacteroides uniformis CECT 7771 ameliorates metabolic and immunological dysfunction in mice with high-fat-diet induced obesity. *PLoS ONE* 7(7):e41079.
- van Passel MW, et al. (2011) The genome of *Akkermansia muciniphila*, a dedicated intestinal mucin degrader, and its use in exploring intestinal metagenomes. *PLoS ONE* 6(3):e16876.
- Cani PD, et al. (2007) Selective increases of bifidobacteria in gut microflora improve high-fat-diet-induced diabetes in mice through a mechanism associated with endotoxaemia. *Diabetologia* 50(11):2374–2383.
- Greenblum S, Turnbaugh PJ, Borenstein E (2012) Metagenomic systems biology of the human gut microbiome reveals topological shifts associated with obesity and inflammatory bowel disease. *Proc Natl Acad Sci USA* 109(2):594–599.
- Vaishnava S, et al. (2011) The antibacterial lectin RegIIIgamma promotes the spatial segregation of microbiota and host in the intestine. *Science* 334(6053):255–258.
- Rajčić-Stojanović M, Shanahan F, Guarner F, de Vos WM (2013) Phylogenetic analysis of dysbiosis in ulcerative colitis during remission. *Inflamm Bowel Dis* 19(3):481–488.
- Geurts L, et al. (2011) Altered gut microbiota and endocannabinoid system tone in obese and diabetic leptin-resistant mice: impact on apelin regulation in adipose tissue. *Front Microbiol* 2:149.

# Supporting Information

Everard et al. 10.1073/pnas.1219451110

## SI Materials and Methods

**Mice. Experiment 1: Ob/Ob experiments.** For *ob/ob* vs. lean study, 6-wk-old *ob/ob* ( $n = 5$  per group) mice (C57BL/6 background, Jackson Laboratories) were housed in a controlled environment (12-h daylight cycle, lights off at 0600 hours) in groups of two or three mice per cage, with free access to food and water. The mice were fed a control diet (A04) for 16 wk. Cecal content was harvested immersed in liquid nitrogen and stored at  $-80^{\circ}\text{C}$  for further *Akkermansia muciniphila* analysis.

**Experiment 2: Ob-prebiotic study.** Six-week-old *ob/ob* ( $n = 10$  per group) mice (C57BL/6 background, Jackson Laboratories) were housed in a controlled environment (12-h daylight cycle, lights off at 0600 hours) in groups of two mice/cage, with free access to food and water. The mice were fed a control diet (A04) or a control diet supplemented with prebiotics (oligofructose) (10 g/100 g of diet) (Orafti) for 5 wk as previously described (1). This set of mice has been previously characterized by Everard et al. (1).

**Experiment 3: High-fat diet prebiotics experiments.** A set of 10-wk-old C57BL/6J mice (40 mice,  $n = 10$  per group) (Charles River Laboratories) were housed in groups of five mice per cage, with free access to food and water. The mice were fed a control diet (A04) or a control diet supplemented with prebiotics (oligofructose) (Orafti) (0.3 g per mouse per day) added in tap water, or fed a high-fat (HF) diet [60% fat and 20% carbohydrates (kcal/100 g), D12492; Research Diet] or an HF diet supplemented with oligofructose (0.3 g per mouse per day) added in tap water. Treatment continued for 8 wk.

**Experiment 4: HF diet *A. muciniphila* treatment.** A set of 10-wk-old C57BL/6J mice (40 mice,  $n = 10$  per group) (Charles River Laboratories) were housed in groups of 2 mice per cage (filter-top cages), with free access to food and water. The mice were fed a control diet (AIN93Mi; Research Diet) or an HF diet [60% fat and 20% carbohydrates (kcal/100 g), D12492; Research Diet]. *A. muciniphila* was daily administered by oral gavage at the dose  $2.10^8$  cfu/0.2 mL suspended in sterile anaerobic PBS (HF-Akk). Treatment continued for 4 wk. Control and HF groups were treated daily with an oral gavage of an equivalent volume of sterile anaerobic PBS for 4 wk. In all cases the sterile anaerobic PBS (pH 7) was supplemented with 0.05% cysteine-HCl, degassed with  $\text{N}_2$ , sealed in serum bottles with butyl rubber stoppers under anaerobic conditions provided by a gas phase of 1.8 atm  $\text{N}_2/\text{CO}_2$  (80:20, vol/vol); this is referred as sterile anaerobic PBS.

*A. muciniphila* MucT (ATCC BAA-835) was grown anaerobically in a basal mucin-based medium as previously described (2). The cultures were washed and concentrated in anaerobic PBS that included 25% (vol/vol) glycerol (reduced with one drop of 100 mM titanium citrate) to an end concentration of  $1.10^{10}$  cfu/mL under strict anaerobic conditions. Subsequently, the cultures were immediately frozen and stored at  $-80^{\circ}\text{C}$ . A representative glycerol stock was thawed under anaerobic conditions to determine the cfu/mL by plate counting using mucin media containing 1% agarose (agar noble; Difco). Before administration by oral gavage, the glycerol stocks were thawed under anaerobic conditions and diluted with anaerobic PBS to an end concentration of  $2.10^8$  viable cfu/0.2 mL. *A. muciniphila* was inoculated in its basal media as previously described (2), supplemented with Casitone (8 g/L) (Bacto Casitone; BD), and oligofructose (50 g/L) as sole carbon source. The growth was analyzed in triplicate by measuring absorbance at 600 nm. No growth was observed.

**Experiment 4: HFD *A. muciniphila* alive vs. heat-killed and *Lactobacillus plantarum* WCFS1.** A set of 10-wk-old C57BL/6J mice (40 mice,  $n = 8$  per group) (Charles River Laboratories) were housed in

groups of 2 mice per cage (filter-top cages), and mice had free access to food and water. The mice were fed the same control diet or an HF diet as described above. *A. muciniphila* was daily administered by oral gavage at the dose  $2.10^8$  cfu/0.2 mL suspended in sterile anaerobic PBS. *A. muciniphila* was heat-killed by autoclaving (15 min,  $121^{\circ}\text{C}$ , 225 kPa). A viability check by culturing on mucin-containing medium confirmed the absence of any viable cells. *Lactobacillus plantarum* WCFS1 was grown anaerobically in MRS medium (Difco Lactobacilli MRS broth; BD), washed, concentrated, and manipulated an identical way as the *A. muciniphila* preparation. The two control groups (CT and HF) were treated daily with an oral gavage of an equivalent volume of sterile anaerobic PBS containing a similar end concentration of glycerol (2.5%) (reduced with one drop of 100 mM titanium citrate) as the treatment groups for 4 wk. The viability of *A. muciniphila* was confirmed by serially diluting the cecal and fecal content immediately postmortem in anaerobic basal mucin-based medium (2) and confirmed with *A. muciniphila*-specific PCR primers (detailed below).

Food and water intake were recorded once per week. Pellets and spillage were weighed separately. Values for the weekly assessment were calculated on the basis of two mice per cage and five cages per group ( $n = 10$  mice per group); the data were reported as cumulative food intake per mouse.

Body composition was assessed by using 7.5 MHz time domain-NMR (LF50 minispec; Bruker).

All mouse experiments were approved by and performed in accordance with the guidelines of the local ethics committee. Housing conditions were specified by the Belgian Law of April 6, 2010, regarding the protection of laboratory animals (agreement number LA1230314).

**Tissue Sampling.** The animals were anesthetized with isoflurane (Forene; Abbott) before exsanguination and tissue sampling, then mice were killed by cervical dislocation. Adipose depots (epididymal, s.c., and mesenteric) and liver were precisely dissected and weighed; the addition of the three adipose tissues corresponds to the adiposity index. The intestinal segments (ileum, cecum, and colon), cecal content, and adipose tissues were immersed in liquid nitrogen and stored at  $-80^{\circ}\text{C}$  for further analysis.

**Mucus Layer Thickness.** Proximal colon segments were immediately removed and fixed in Carnoy's solution (ethanol 6: acid acetic 3: chloroform 1, vol/vol) for 2 h at  $4^{\circ}\text{C}$ . They were then immersed in ethanol 100% for 24 h. Paraffin sections of  $5\ \mu\text{m}$  were stained with alcian blue. A minimum of 20 different measurements were made perpendicular to the inner mucus layer per field. Five to nineteen randomly selected fields were analyzed for each colon for a total of 4,549 measurements by using an image analyzer (Motic-image Plus 2.0ML; Motic).

**RNA Preparation and Real-Time Quantitative PCR Analysis.** Total RNA was prepared from tissues using TriPure reagent (Roche). Quantification and integrity analysis of total RNA was performed by running  $1\ \mu\text{L}$  of each sample on an Agilent 2100 Bioanalyzer (Agilent RNA 6000 Nano Kit). cDNA was prepared by reverse transcription of  $1\ \mu\text{g}$  total RNA using a Reverse Transcription System Kit (Promega). Real-time PCRs were performed with the StepOnePlus real-time PCR system and software (Applied Biosystems) using Mesa Fast qPCR (Eurogentec) for detection according to the manufacturer's instructions. RPL19 RNA was chosen as the housekeeping gene. All samples were run in

duplicate in a single 96-well reaction plate, and data were analyzed according to the  $2^{-\Delta CT}$  method. The identity and purity of the amplified product was checked through analysis of the melting curve carried out at the end of amplification. Primer sequences for the targeted mouse genes are presented in Table S1.

**Insulin Resistance Index.** Insulin resistance index was determined by multiplying the area under the curve (0 min and 15 min) of both blood glucose and plasma insulin obtained after an oral glucose load (2 g of glucose per kg of body weight) performed after 4 wk (*A. muciniphila* study) of treatment. Food was removed 2 h after the onset of the daylight cycle, and mice were treated after a 6-h fasting period as previously described (1).

**Biochemical Analyses.** Portal vein blood LPS concentration was measured using an Endosafe-Multi-Cartridge System (Charles River Laboratories) based on the *Limulus* amoebocyte lysate (LAL) kinetic chromogenic methodology that measures color intensity directly related to the endotoxin concentration in a sample. Serum were diluted 1/10 with endotoxin-free buffer to minimize interferences in the reaction (inhibition or enhancement) and heated 15 min at 70 °C. Each sample was diluted 1/70 or 1/100 with endotoxin-free LAL reagent water (Charles River Laboratories) and treated in duplicate, and two spikes for each sample were included in the determination. All samples have been validated for the recovery and the coefficient variation. The lower limit of detection was 0.005 EU/mL. Plasma insulin concentration was determined in 25  $\mu$ L of plasma using an ELISA kit (Merckodia) according to the manufacturer instructions.

**DNA Isolation from Mouse Cecal Samples.** The cecal content of mice collected postmortem was stored at  $-80$  °C. Metagenomic DNA was extracted from the cecal content using a QIAamp-DNA stool minikit (Qiagen) according to the manufacturer's instructions.

- Everard A, et al. (2011) Responses of gut microbiota and glucose and lipid metabolism to prebiotics in genetic obese and diet-induced leptin-resistant mice. *Diabetes* 60(11): 2775–2786.
- Derrien M, Vaughan EE, Plugge CM, de Vos WM (2004) *Akkermansia muciniphila* gen. nov., sp. nov., a human intestinal mucin-degrading bacterium. *Int J Syst Evol Microbiol* 54(Pt 5):1469–1476.

**Measurement of Endocannabinoids Intestinal Levels.** Ileum tissues were homogenized in  $\text{CHCl}_3$  (10 mL), and a deuterated standards (200 pmol) were added. The extraction and the calibration curves were generated as previously described (3), and the data were normalized by tissue sample weight.

**qPCR: Primers and Conditions.** The primers and probes used to detect *A. muciniphila* were based on 16S rRNA gene sequences: forward *A. muciniphila*, CAGCACGTGAAGGTGGGGAC, reverse *A. muciniphila*, CCTTGCGGTTGGCTTCAGAT. Detection was achieved with StepOnePlus real-time PCR system and software (Applied Biosystems) using Mesa Fast qPCR (Eurogentec) according to the manufacturer's instructions. Each assay was performed in duplicate in the same run. The cycle threshold of each sample was then compared with a standard curve (performed in triplicate) made by diluting genomic DNA (fivefold serial dilution) (DSMZ). The data are expressed as log of bacteria per g of cecal content.

**Mouse Intestinal Tract Chip: PCR Primers and Conditions.** The Mouse Intestinal Tract Chip (MITChip) is a phylogenetic microarray consisting of 3,580 different oligonucleotides specific for the mouse intestinal microbiota. Both the design and analysis of the MITChip were performed as previously described (1, 4).

**Statistical Analysis.** Data are expressed as means  $\pm$  SEM. Differences between two groups were assessed using the unpaired two-tailed Student *t* test. Data sets involving more than two groups were assessed by ANOVA followed by Newman-Keuls post hoc tests after normalization by log transformation. Correlations were analyzed using Pearson's correlation. Data with different superscript letters are significantly different  $P < 0.05$ , according to post hoc ANOVA statistical analysis. Data were analyzed using GraphPad Prism version 5.00 for windows (GraphPad Software). Results were considered statistically significant when  $P < 0.05$ .

- Muccioli GG, et al. (2010) The endocannabinoid system links gut microbiota to adipogenesis. *Mol Syst Biol* 6:392.
- Geurts L, et al. (2011) Altered gut microbiota and endocannabinoid system tone in obese and diabetic leptin-resistant mice: Impact on apelin regulation in adipose tissue. *Front Microbiol* 2:149.

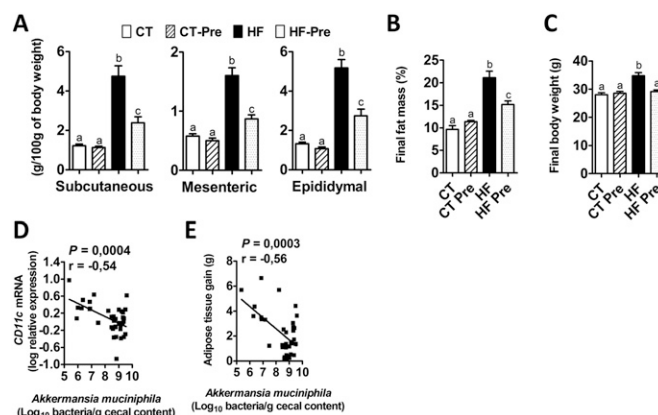


**Fig. S1.** Prebiotic-treated mice on an HF diet exhibited a decrease in s.c., mesenteric, and epididymal fat mass and in body weight. (A) s.c., mesenteric, and epididymal fat depot weights (g per 100 g body weight) measured in control diet-fed mice (CT), control diet-fed mice treated with prebiotics (CT-Pre), HF diet-fed mice (HF), and HF diet-fed mice treated with prebiotics (HF-Pre) ( $n = 10$ ). (B) Final fat mass expressed in percentage of final body weight and measured by time-domain NMR ( $n = 10$ ). (C) Final body weight ( $n = 10$ ). (D) Pearson's correlation between adipose tissue *CD11c* mRNA levels and *A. muciniphila* abundance ( $\log_{10}$  of bacteria per g of cecal content) measured in the cecal content; (Inset) Pearson's correlation coefficient ( $r$ ) and the corresponding  $P$  value. (E) Pearson's correlation between adipose tissue mass gain and cecal content of *A. muciniphila* ( $\log_{10}$  of bacteria per g of cecal content); (Inset) Pearson's correlation coefficient ( $r$ ) and the corresponding  $P$  value. Data are shown as means  $\pm$  SEM. Data with different superscript letters are significantly different ( $P < 0.05$ ) according to post hoc ANOVA one-way statistical analysis.



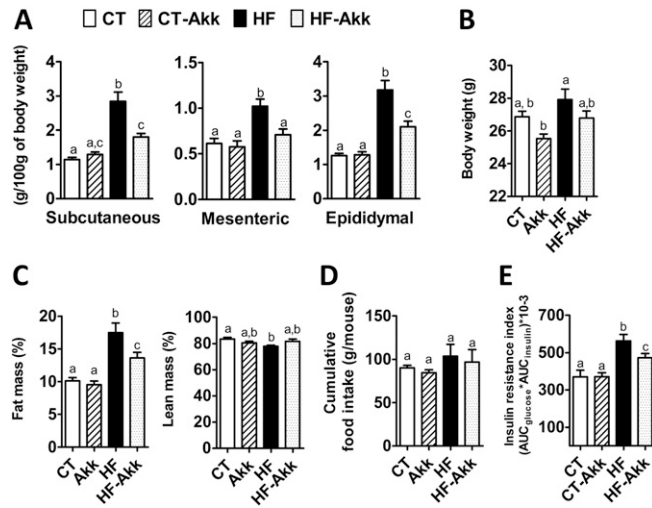


**Fig. S3.** *A. muciniphila* treatment reduced s.c., mesenteric, and epididymal fat mass, body weight, and insulin resistance in mice on an HF diet without affecting food intake. (A) s.c., mesenteric, and epididymal fat depot weights (g per 100 g body weight) measured in mice treated daily with an oral gavage of *A. muciniphila* and fed a control (CT-Akk) or HF diet (HF-Akk) or mice fed a control (CT) or HF diet and treated daily with an oral gavage of sterile anaerobic PBS ( $n = 10$ ). (B) Final body weight ( $n = 10$ ). (C) Final fat and lean mass expressed in percentage of final body weight and measured by time-domain NMR ( $n = 10$ ). (D) Cumulative food intake (g) over the 4 wk of treatment. (E) Insulin resistance index was determined by multiplying the area under the curve (from 0 min to 15 min) of blood glucose and plasma insulin that were obtained after an oral glucose load (2 g glucose per kg of body weight) after 4 wk of treatment ( $n = 10$ ). Data are shown as means  $\pm$  SEM. Data with different superscript letters are significantly different ( $P < 0.05$ ) according to post hoc ANOVA one-way statistical analysis.

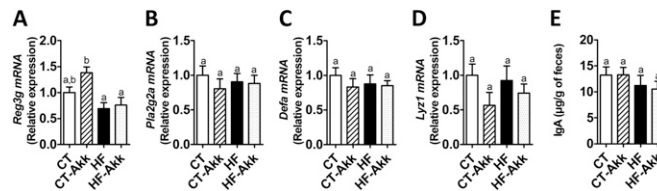


**Fig. S4.** *A. muciniphila* treatment exerted minor effects on antibacterial peptide contents in the ileum and IgA levels in the feces. Antibacterial peptide mRNA expression: (A) regenerating islet-derived 3- $\gamma$  (RegIII $\gamma$ , encoded by *Reg3g*), (B) phospholipase A2 group IIA (encoded by *Pla2g2a*), (C)  $\alpha$ -defensins (encoded by *Defa*), and (D) lysozyme C (encoded by *Lyz1*) measured in the ileum of mice treated daily with an oral gavage of *A. muciniphila* ( $2.10^8$  bacterial cells suspended in 200  $\mu$ L of sterile anaerobic PBS) and fed a control (CT-Akk) or HF-diet (HF-Akk) or mice fed a control (CT) or HF diet and treated daily with an oral gavage of an equivalent volume of sterile anaerobic PBS for 4 wk ( $n = 10$ ). (E) Fecal IgA levels ( $\mu$ g/g of feces). Data are shown as means  $\pm$  SEM. Data with different superscript letters are significantly different ( $P < 0.05$ ) according to post hoc ANOVA one-way statistical analysis.

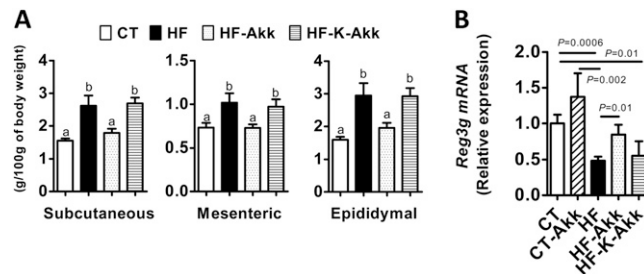


**Fig. S5.** Heat-Killed *A. muciniphila* did not reduce s.c., mesenteric, and epididymal fat mass and did not increase colon antimicrobial peptides in mice on an HF diet. (A) s.c., mesenteric, and epididymal fat depot weights (g per 100 g body weight) measured in control mice fed a control (CT) or HF diet (HF) and treated with a daily oral gavage containing sterile anaerobic PBS and glycerol for 4 wk daily. Treated mice received an oral gavage of alive *A. muciniphila* (HF-Akk) or killed *A. muciniphila* (HF-K-Akk) ( $2.10^8$  bacterial cells suspended in 200  $\mu$ L of sterile anaerobic PBS) and fed a HF diet ( $n = 8$ ). (B) mRNA expression of colon RegIII $\gamma$  (encoded by *Reg3g*) mRNA expression ( $n = 8$ –18); data represent the results from the two *A. muciniphila* studies. Data are shown as means  $\pm$  SEM. Data with different superscript letters are significantly different ( $P < 0.05$ ) according to post hoc ANOVA one-way statistical analysis.

